JOURNAL OF VIROLOGY, Apr. 2009, p. 3019–3028 Vol. 83, No. 7
0022-538X/09/$08.00+0 doi:10.1128/JVI.00036-09

# Regulatory T Cells Promote Early Influx of CD8$^+$ T Cells in the Lungs of Respiratory Syncytial Virus-Infected Mice and Diminish Immunodominance Disparities$^{\nabla}$†

Tracy J. Ruckwardt,[1] Kathryn L. Bonaparte,[1] Martha C. Nason,[2] and Barney S. Graham[1]*

*Viral Pathogenesis Laboratory, Vaccine Research Center, National Institute of Allergy and Infections Diseases, National Institutes of Health, Bethesda, Maryland,[1] and Biostatistics Research Branch, National Institute of Allergy and Infections Diseases, National Institutes of Health, Bethesda, Maryland[2]*

Received 5 December 2008/Accepted 9 January 2009

**In addition to regulating autoimmunity and antitumor immunity, CD4$^+$ CD25$^+$ FoxP3$^+$ natural regulatory T (Treg) cells are global regulators of adaptive immune responses. Depletion of these cells with the anti-CD25 antibody PC61 prior to primary respiratory syncytial virus (RSV) infection was partial but had several effects on the RSV-specific CD8$^+$ response in a hybrid mouse model. Mediastinal lymph node and spleen epitope-specific CD8$^+$ T-cell responses were enhanced in Treg-cell-depleted mice at all time points following infection, but responses of Treg-cell-depleted lung show a strikingly different pattern than lymphoid organ responses, with an initial delay in the CD8$^+$ T-cell response. The delay in the CD8$^+$ T-cell response correlated with a delay both in the early phase of viral clearance and in illness in Treg-cell-depleted mice compared to isotype-treated controls. The lungs of Treg-cell-depleted mice were shown to have increased lung chemokine and cytokine levels 7 days postinfection despite lower CD8$^+$ T-cell responses. Following the early delay in the lung response, CD8$^+$ T-cell responses at later infection time points were enhanced and increased the severity of illness in depleted mice. Finally, decreasing regulatory T-cell control of the CD8$^+$ T-cell response had a greater effect on response of the dominant K$^d$-restricted M2 epitope consisting of amino acids 82 to 90 (K$^d$M2$_{82–90}$) than on the subdominant D$^b$M$_{187–195}$ epitope response, indicating that regulatory T cells modulate immunodominance disparities in epitope-specific CD8$^+$ T-cell responses following primary RSV infection.**

Natural regulatory T (Treg) cells are among a growing family of T-cell subsets found to have a negative regulatory effect on immune responses (1, 24, 31–33, 36). These cells represent 5 to 10% of all CD4$^+$ T cells in the mouse and are characterized by the expression of FoxP3, a transcription factor determining regulatory cell lineage development (14). Most Treg cells also express the high-affinity interleukin-2 (IL-2) receptor CD25, and IL-2 has been shown to be critical for Treg-cell maintenance and function (41). CD8$^+$ T-cell effector functions and proliferation are often dampened by negative regulation by Treg cells (31, 32). Anti-CD25 antibody depletion studies in the mouse show increased CD8$^+$ T-cell responses following depletion of Treg cells and often increased clearance of the pathogen (8, 9, 12, 29, 39, 40).

We have characterized the immune response to respiratory syncytial virus (RSV) in the CB6F1 hybrid mouse, where both the *d*-allele-restricted dominant epitope in the M2 protein (amino acids 82 to 90 [K$^d$M2$_{82–90}$]) and *b*-allele-restricted subdominant epitope (D$^b$M$_{187–195}$) responses can be studied simultaneously (19, 34, 35). This model allows us to look at the relative contribution of epitope-specific CD8$^+$ T-cell responses to viral clearance and illness and investigate factors involved in the establishment of epitope hierarchy. Both viral clearance and illness in RSV-infected mice are intrinsically tied to the CD8$^+$ T-cell response (10). The K$^d$M2$_{82–90}$ epitope response dominates during primary RSV infection of CB6F1 mice, representing up to 50% of CD8$^+$ T cells in the lungs. The D$^b$M$_{187–195}$ epitope is the next dominant response, representing up to 15%, with other described *d* and *b* allele epitopes (4, 21, 22) representing a small fraction of the responding CD8$^+$ T-cell response in lungs of RSV-infected CB6F1 mice.

Given the suppressive potential of Treg cells during viral infections, we hypothesized that depletion of Treg cells prior to intranasal infection with RSV would facilitate viral clearance from the lungs yet increase illness due to CD8$^+$-mediated immunopathology. Surprisingly, we found that animals that were Treg cell depleted experienced less efficient RSV clearance and a delay in CD8$^+$ T-cell responses in the lung despite increased levels of RSV-specific CD8$^+$ T cells in the lung-draining lymph node and spleen early after infection. However, increased cytokine and chemokine expression 7 days postinfection and exaggerated CD8$^+$ T-cell responses in the lung after the first week of infection resulted in a later exacerbation of disease and slower recovery from illness. Treg-cell depletion not only altered the kinetics of the CD8$^+$ T-cell response but also resulted in systemic modulation of the immunodominance disparity between the K$^d$M2$_{82–90}$ and the D$^b$M$_{187–195}$ epitopes.

## MATERIALS AND METHODS

**Mice.** Adult (6- to 10-week-old) female CB6F1 mice (Jackson Laboratories, Bar Harbor, ME) were used for all experiments. All mice were housed in our animal care facility at the National Institute of Allergy and Infections Diseases under specific-pathogen-free conditions and maintained on standard rodent

* Corresponding author. Mailing address: Vaccine Research Center, National Institute of Allergy and Infections Diseases, National Institutes of Health, 40 Convent Dr., Bethesda, MD 20892. Phone: (301) 594-8468. Fax: (301) 480-2771. E-mail: bgraham@nih.gov.

† Supplemental material for this article may be found at http://jvi.asm.org/.

$^{\nabla}$ Published ahead of print on 19 January 2009.

chow and water supplied ad libitum. All studies were reviewed and approved by the NIH Animal Care and Use Committee.

**Cell lines and antibodies.** HEp-2 cells were used to determine titers of RSV from lungs. Cells were maintained in Eagle's minimal essential medium containing 10% fetal bovine serum (10% EMEM) and were supplemented with 2 mM glutamine, 10 U of penicillin G per ml, and 10 μg of streptomycin sulfate per ml. Cells were determined to be free of mycoplasma contamination by analysis with the PCR (ATCC, Manassas, VA).

The hybridoma-producing anti-mouse CD25 was a kind gift from J. Yewdell, and purified monoclonal antibody was manufactured by Harlan (Indianapolis, IN).

**Viruses and infection.** The RSV challenge stock was derived from the A2 strain of RSV by sonication of HEp-2 monolayers as previously described (11). Mice were anesthetized intramuscularly with ketamine (40 μg/g of body weight) and xylazine (6 μg/g of body weight) prior to intranasal inoculation with $6 \times 10^6$ PFU of live RSV in 100 μl of 10% EMEM. Mice were weighed daily after infection, and percent weight lost was used to assess the severity of illness.

**Plaque assays.** Mice were sacrificed, and lung tissue was removed and quick frozen in 10% EMEM. Thawed tissues were kept chilled while individually ground. Dilutions of clarified supernatant were inoculated on 80% confluent HEp-2 cell monolayers in triplicate and overlaid with 0.75% methyl cellulose in 10% EMEM. After incubation for 4 days at 37°C, the monolayers were fixed with 10% buffered formalin and stained with hematoxylin and eosin. Plaques were counted and expressed as $\log_{10}$ PFU/gram of tissue. The limit of detection is 1.8 $\log_{10}$ PFU/gram of tissue.

**Synthetic peptides.** RSV $M2_{82–90}$ (SYIGSINNI) and RSV $M_{187–195}$ (NAITN AKII) were derived from the M2 and M proteins, respectively, of the RSV A2 strain (19, 34). An H2-$K^d$-binding influenza virus A/Puerto Rico/8/34 nucleoprotein peptide comprised of residues 147 to 155 ($NP_{147–155}$; TYQRTRALV) and an H2-$D^b$-binding influenza A/Puerto Rico/8/34 peptide $NP_{366–374}$ (ASNENM ETM) were used as negative controls. All peptides were synthesized by Anaspec, Inc. (San Jose, CA), and confirmed to be >95% pure by analytical high-performance liquid chromatography at the National Institute of Allergy and Infections Diseases peptide core facility (Bethesda, MD).

**Class I tetramers.** Tetramers were synthesized by Beckman Coulter (San Diego, CA). Virus-specific T cells were enumerated with phycoerythrin-labeled tetrameric complexes of H-$2K^d$ plus the RSV $M2_{82–90}$ peptide or allophycocyanin-labeled tetrameric complexes of H-$2D^b$ plus the RSV $M_{187–195}$ peptide. For negative controls, cells from uninfected mice were stained, and phycoerythrin-labeled tetrameric complexes of H-$2D^b$ with the influenza virus $NP_{366–374}$ peptide, H-$2K^d$ with the influenza virus $NP_{147–155}$ peptide, or H-$2K^b$ with an ovalbumin epitope comprised of residues 257 to 264 ($Ova_{257–264}$; SIINFEKL) were used.

**Tetramer and intracellular cytokine staining (ICS).** Mice were sacrificed, and lungs, lymph nodes, and spleens were harvested at various times between days 4 and 14 postinfection. Spleens were also harvested 60 to 100 days postinfection to analyze memory responses. Lymphocytes were isolated manually by grinding organ tissue between the frosted ends of two sterile glass microscope slides in RPMI medium containing 10% fetal bovine serum. Lymphocytes were isolated by centrifugation on a cushion of Fico/Lite-LM at room temperature, washed, and resuspended in RPMI medium containing 10% fetal bovine serum. Lymphocytes were incubated at 37°C for 5 h with 1 μg of the appropriate peptide, 1 μg/ml of the costimulatory antibodies against CD28 and CD49d, and 1 μg/ml of monensin to retain newly synthesized proteins within the cell. As a positive control, cells were stimulated with 10 ng/ml phorbol myristate acetate and 1 μM ionomycin. After the incubation, cells were surface stained with antibodies against CD3 (145-2C11), CD4 (GK1.5), and CD8 (2.43) and then fixed and permeabilized according to the manufacturer's instructions (BD Pharmingen, San Diego, CA). Intracellular stains were done with antibodies to gamma interferon ([IFN-γ] XMG1.2), IL-2 (JES6-5H4), and tumor necrosis factor alpha ([TNF-α] MP6-XT22) (BD Pharmingen) for 20 min at 4°C. For tetramer analysis, cells were stained with tetramer against $D^bM_{187–195}$ or $K^dM2_{82–90}$ in addition to antibodies against CD3, CD4, and CD8; for Treg-cell analysis, cells were stained for CD3, CD4, CD8, and CD25 (7D4) expression and then permeabilized before staining with anti-FoxP3 (FJK-16S). Tetramers that recognized the influenza virus $NP_{366–374}$ epitope or the SIINFEKL Ova epitope were used as negative controls. After cells were stained, they were washed and analyzed by flow cytometry. Cell samples were run on an LSR II instrument (Becton Dickinson, San Jose, CA). Data were analyzed by using FlowJo software, version 8.5 (Tree Star, San Carlos, CA). Gating for flow cytometry analysis is shown in Fig. S1 in the supplemental material. Intracellular cytokine samples were Boolean gated following single positive cytokine gating and then background subtracted in Pestle (software provided by Mario Roederer, Bethesda, MD) prior to graphing.

**Chemokine and cytokine analysis.** Frozen, ground lung supernatant samples were shipped to the SearchLight sample testing service provided by Pierce (http://www.piercenet.com/) for multiplex proteome analysis of mouse cytokines.

**Statistical analysis.** Linear regression was used to analyze the differences between control and depleted mice in the ratio of $K^dM2_{82–90}/D^bM_{187–195}$ responses over time, separately for the lung, spleen, and lymph nodes. For each organ, a model was fit with the log10 of the ratio as the response variable and predictors consisting of main effects for the study day and depletion status. These models also included an interaction between depletion status and study day to allow for a different slope in the two groups of mice. To explore the appropriateness of the ratio as a response variable, additional linear models were fit to the log of the $K^dM2_{82–90}$ values, including the predictors as above, and the $D^bM_{187–195}$ value (also on the log scale) for each mouse. Since the results were very similar for both sets of models, we focused on the results of the models for the ratio of $K^dM2_{82–90}/D^bM_{187–195}$. Standard model-checking procedures were followed to assess fit; no inconsistencies were seen with the exception of one outlier in the lymph node data, in which the $K^dM2_{82–90}$ value was substantially higher (10-fold) than for any other mouse. To determine if this point was overly influential in our modeling and conclusions, we refit the models to the lymph node data with the outlier removed. Neither the estimates of treatment effects nor the significance of these effects changed significantly when this point was removed.

For other data, a two-tailed Student's *t* test was used for statistical analysis, and *P* values of $<0.05$ were considered statistically significant.

## RESULTS

**Treg cells are enriched in RSV-infected lungs and are partially depleted with PC61 (anti-CD25) antibody.** Treg cells are often found to respond to infection and inflammation (2, 32, 33). We first investigated the extent of the Treg-cell response during primary RSV infection in both isotype antibody-treated CB6F1 mice and mice depleted of Treg cells with the anti-CD25 antibody PC61. In mice treated with isotype antibody, Treg-cell numbers nearly tripled, rising from 5.4% of lymphocytes in uninfected mouse lungs to 13.4% in RSV-infected lungs and peaking at 6 to 7 days postinfection ($P = 0.048$) (Fig. 1A). Antibody-mediated depletion with the PC61 primarily depleted $CD4^+$ $CD25^+$ $FoxP3^+$ cells from the lungs, as previously reported in other model systems, and had little to no effect on the percentage of $CD4^+$ $CD25^-$ $FoxP3^+$ cells (6). This partial depletion was sufficient to inhibit much of the early influx of Treg cells in the RSV-infected lung, though Treg-cell percentages in the lung were still significantly higher at day 6 postinfection than in uninfected, depleted mice ($P = 0.016$). However, even following RSV infection, Treg-cell-depleted mice had a significantly lower percentage of Treg cells in the lungs than control isotype-treated mice at all time points. The response in depleted mice peaked at 5.7% at 6 days postinfection, just above the level found in the lungs of uninfected mice.

Treg cells represented close to 10% of $CD4^+$ T cells in the spleen of uninfected mice and did not significantly change throughout the course of infection in isotype control-treated mice. Treg-cell depletion was sufficient to reduce the number of Treg cells in the spleen by nearly 50%, with primarily $CD25^-$ $FoxP3^+$ cells remaining (Fig. 1B). Mediastinal (lung-draining) lymph nodes were not visible in uninfected mice or early after infection, but samples taken starting 6 days postinfection indicated percentages of Treg cells similar to the numbers in spleen in both control and depleted mice (Fig. 1C), showing again a reduction of nearly 50%. Comparing the percentages of Treg cells in the lungs, spleen, and lymph node indicated a clear enrichment of Treg cells in the lungs following RSV infection but not in the secondary lymphoid organs. A similar pattern was noted for absolute cell numbers as dem-

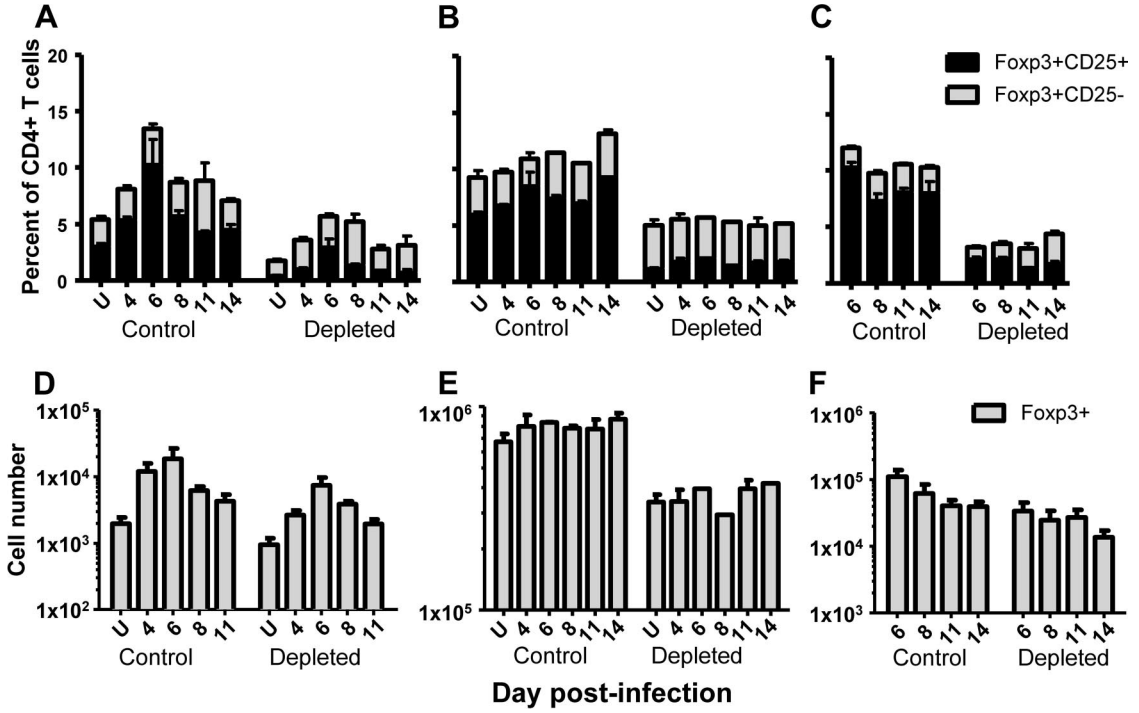


FIG. 1. Total FoxP3$^+$ Treg cells in control and anti-CD25-depleted mice. Mice were treated with 500 μg of isotype antibody (Y13-259; control) or 500 μg of PC61 antibody (depleted) intraperitoneally 3 days prior to intranasal infection with $6 \times 10^6$ PFU of RSV. Percentages of FoxP3$^+$ cells that are CD25$^+$ or CD25$^-$ are shown in the lung (A), spleen (B), and mediastinal lymph node (C) samples at the given day postinfection with RSV. U designates the same organ samples from antibody-treated, uninfected mice. Absolute numbers of FoxP3$^+$ cells are shown through day 11 for the right lung (D) and through day 14 for spleen (E) and mediastinal lymph nodes (F). Both right and left lungs were analyzed on day 14, and so that time point was not included in panel D. Error bars represent the standard error of the mean with four mice per group, and the experiment was repeated with similar results.

onstrated by CD4$^+$ FoxP3$^+$ T cells in lung (Fig. 1D), spleen (Fig. 1E), and mediastinal lymph nodes (Fig. 1F).

Activated CD8$^+$ and CD4$^+$ T cells may also express CD25; therefore anti-CD25 could potentially have nonspecific effects on these populations. We measured CD25 expression on CD8$^+$ T cells and CD4$^+$ FoxP3$^-$ T cells in the lung, lymph node, and spleen following primary RSV infection. Overall, very few CD8$^+$ T cells in the lymph node and spleen express CD25, and only small percentages express it in the lung (Fig. 2A). Similarly, almost all CD4$^+$ FoxP3$^-$ cells do not express CD25 in the lymph node and spleen, and few cells do so in the lung (Fig. 2B). PC61 depletion had little effect on CD25$^+$ expression in either the CD8$^+$ or the CD4$^+$ FoxP3$^-$ populations.

**Treg-cell depletion delays the rate of viral clearance and illness early in infection but results in increased disease severity at later time points.** Viral titer in the lungs of RSV-infected CB6F1 mice peaks 4 to 5 days following infection (Fig. 3A). Surprisingly, Treg-cell-depleted mice did not clear RSV from the lungs as efficiently as control mice. Depleted mice demonstrated 1 to 2 logs more virus in the lungs 6 to 7 days postinfection than isotype control-treated mice that more efficiently cleared virus (Fig. 3A). The most dramatic difference between the control and Treg-cell-depleted groups was seen on day 6 ($P = 0.0009$). Despite these kinetic differences in the onset of viral clearance, both control and Treg-cell-depleted mice achieved viral clearance (below the lowest detectable level of 1.8 logs) by 8 days following infection.

The early lag in viral clearance in Treg-cell-depleted mice correlated with a delay in illness, as measured by percent weight loss at day 6 ($P = 0.0026$) (Fig. 3B). After day 7 postinfection, Treg-cell-depleted mice experienced more severe and sustained weight loss than isotype control-treated mice, with significant differences at days 9 ($P = 0.02$) and 10 ($P = 0.01$) postinfection (Fig. 3B). Multiple statistical comparisons were used, and weight loss was reproducible between duplicate experiments.

**Depletion of Treg cells prior to RSV infection alters the kinetics of the CD8$^+$ T-cell response and exaggerates epitope dominance disparities.** We were intrigued by the delay in the early phase of viral clearance in Treg-cell-depleted mice, given several published reports of increased pathogen-specific CD8$^+$ T-cell responses, which are responsible for RSV clearance from the lungs. We therefore assessed RSV-specific CD8$^+$ T-cell responses in the lungs of RSV-infected CB6F1. CB6F1 mice are *H-2*$^{d/b}$, allowing us to perform tetramer staining for both the dominant $K^dM2_{82-90}$ epitope and the subdominant $D^bM_{187-195}$ epitope. Both of these adaptive T-cell responses are absent in the lungs at 4 days postinfection and are detectable by day 6. We were surprised to find a higher percentage of both $K^dM2_{82-90}$-specific cells (Fig. 4A) and $D^bM_{187-195}$-specific cells (Fig. 4D) in the lungs of the isotype control group

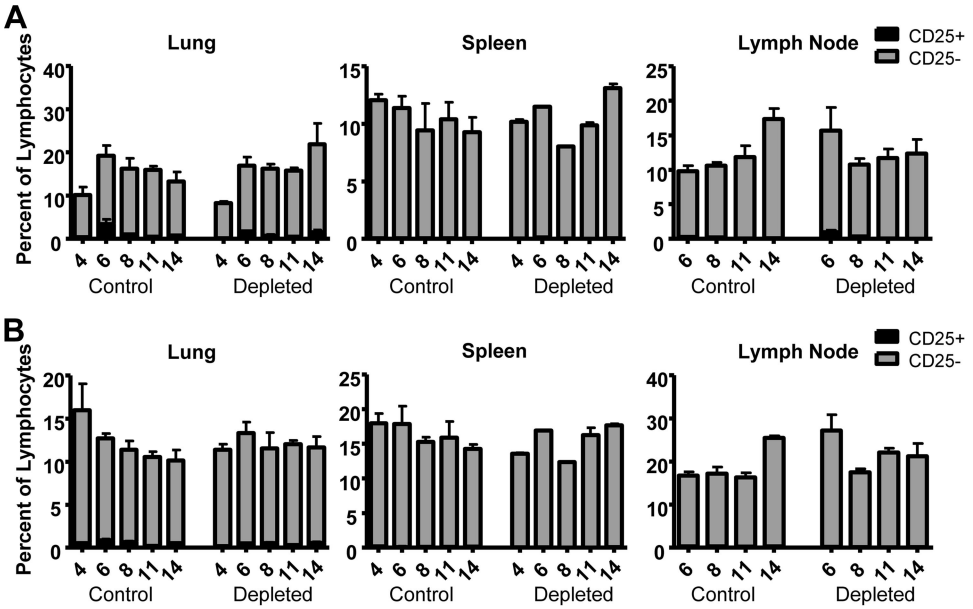


FIG. 2. $CD25^+$ expression on $CD8^+$ and $CD4^+$ $FoxP3^-$ T cells in control and anti-CD25-depleted mice. Mice were treated with 500 μg of isotype antibody (Y13-259; control) or PC61 antibody (depleted) 3 days prior to infection at day 0. $CD25^+$ expression was measured on $CD8^+$ T cells (A) and on $CD4^+$ $FoxP3^-$ T cells (B) in the lung, lymph node, and spleen by flow cytometry following primary infection with RSV. Error bars represent the standard error of the mean with four mice per group, and the experiment was performed two times.

than in the Treg-cell-depleted group at 6 to 7 days postinfection. The experiment was repeated twice, with the data from both experiments showing a similar early lag in the Treg-cell-depleted group. However, only one experiment resulted in statistically significant differences during early infection (for $K^dM2_{82–90}$ responses, $P = 0.028$; for $D^bM_{187–195}$ responses, $P = 0.009$). The dominant $K^dM2_{82–90}$ response in the Treg-cell-depleted and control groups was the same at 8 days postinfection and was significantly higher in the Treg-cell-depleted group at later infection time points (Fig. 4A). Again, of the two experiments showing the same trend, only one showed statistical differences between the control and Treg-cell-depleted groups during late infection (for $K^dM2_{82–90}$ responses, $P = 0.036$; for $D^bM_{187–195}$ responses, $P = 0.002$). The subdominant $D^bM_{187–195}$ response experienced a greater lag in the lungs of the Treg-cell-depleted group, remaining lower than the isotype control-treated groups through day 11 (Fig. 4D). The delay in both of these RSV epitope-specific $CD8^+$ T-cell responses in the lungs of Treg-cell-depleted mice offered an explanation for inefficient viral clearance and less illness early in infection, and, conversely, higher $CD8^+$ T-cell epitope-specific responses at later infection time points accounted for more severe and sustained weight loss in the Treg-cell-depleted group after day 7.

RSV epitope-specific responses were also measured in the spleen and the mediastinal (lung-draining) lymph node following infection. The spleen showed the greatest difference between the Treg-cell-depleted and control groups for the $K^dM2_{82–90}$ epitope (Fig. 4B). In contrast to what was seen in the lung, responses to $K^dM2_{82–90}$ in isotype-treated mice were

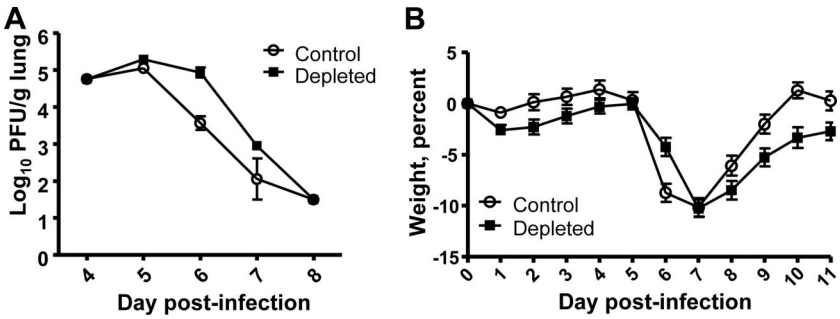


FIG. 3. (A) Lung virus titers in control and anti-CD25-treated mice. Mice were treated with 500 μg of isotype antibody (Y13-259; control) or PC61 antibody (depleted) 3 days prior to infection at day 0. Left lungs were harvested at the indicated day after RSV infection, quick-frozen, and then later ground and plated on HEp-2 cells to determine the number of PFU per gram of tissue harvested. Error bars represent the standard error of the mean with four mice per group, and the experiment was done two times. (B) Illness following RSV infection of control or anti-CD25-depleted mice. Animal weights were taken daily and compared to baseline weights on the day of RSV infection (day 0). The error bars represent the standard error of the mean for 10 mice per group, and the experiment was performed two times.

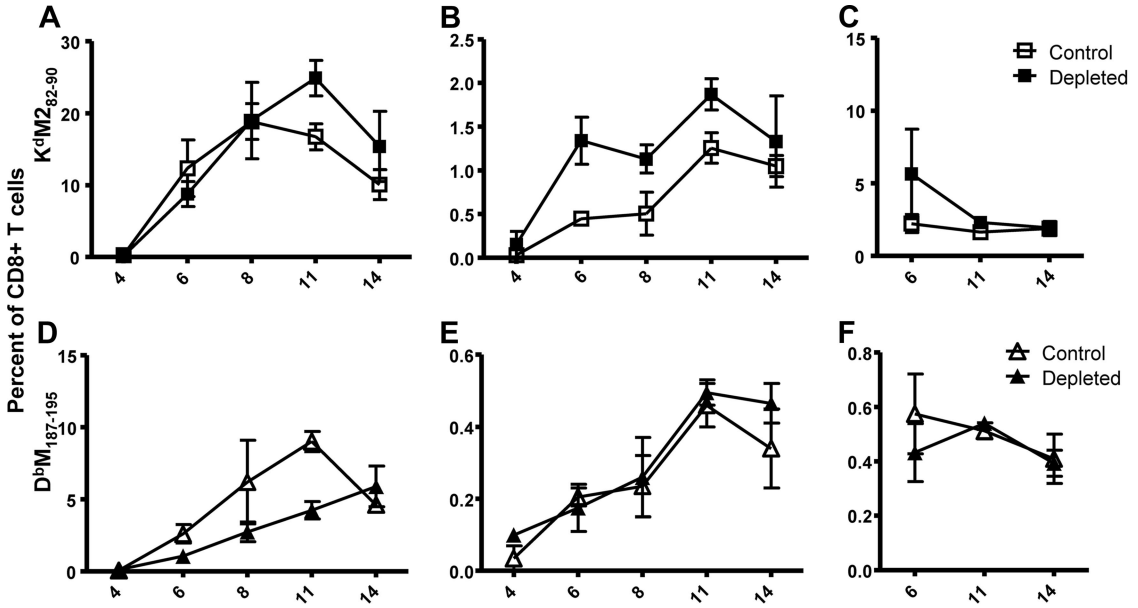


FIG. 4. Kinetics of $K^dM2_{82–90}$ and $D^bM_{187–195}$ epitope-specific responses following RSV infection in control and anti-CD25-treated mice. Mice were treated with 500 μg of isotype antibody (Y13-259; control) or 500 μg of PC61 antibody (depleted) intraperitoneally 3 days prior to intranasal infection with RSV. Percentages of $CD8^+$ T cells specific for the $K^dM2_{82–90}$ epitope or the $D^bM_{187–195}$ epitope were determined in the lungs (A and D), spleens (B and E), and mediastinal lymph nodes (C and F) at the indicated day following RSV infection by surface staining with antibodies against CD3, CD8, and epitope-specific tetramers. The means of total cell numbers between treatment groups were all within 1 standard deviation. Error bars represent the standard error of the mean with four mice per group, and the experiment was done twice.

lower than in Treg-cell-depleted mice at all time points after infection. However, subdominant $D^bM_{187–195}$ epitope responses in the spleen were not significantly different between the isotype control and Treg-cell-depleted groups (Fig. 4E). Finally, significant differences between the $K^dM2_{82–90}$ and $D^bM_{187–195}$ epitope responses were not evident in the mediastinal lymph node, with a slightly higher $K^dM2_{82–90}$ response in the Treg-cell-depleted group and a slightly higher $D^bM_{187–195}$ response in the isotype control group at day 6 only (Fig. 4C and F). Taking into account both epitopes, the total quantity of RSV-specific T cells in secondary lymphoid organs following infection was higher in the Treg-cell-depleted group than in the isotype control group, largely due to a increase in the dominant $K^dM2_{82–90}$ response.

A previous study indicated that Treg cells may have the greatest suppressive effect on the most dominant $CD8^+$ T-cell response, moderating the immunodominance disparity between epitopes (12). We investigated this effect in our RSV mouse model by looking at the ratio of the dominant $K^dM2_{82–90}$ response to the subdominant $D^bM_{187–195}$ response for each infected mouse, thus expressing the relative difference between the two epitope responses. In a comparison of the ratio of $K^dM2_{82–90}$ to $D^bM_{187–195}$ in the lungs of isotype control-treated mice, the dominant $K^dM2_{82–90}$ response was less than fivefold higher than the response to $D^bM_{187–195}$ throughout the entire course of infection. In contrast, in the lungs of Treg-cell-depleted mice the dominant response was ninefold higher at 6 days postinfection and remained higher than the isotype control groups until day 14 postinfection (Fig. 5A). The $K^dM2_{82–90}/D^bM_{187–195}$ ratios in the spleen and mediastinal lymph node of isotype-treated control mice remained lower than 5 throughout the infection (Fig. 5B and C). As seen in the lung, the ratio was significantly higher in Treg-cell-depleted mice for both the spleen and the lymph node, particularly early in the infection (Fig. 5B and C). These data indicate that Treg cells moderate epitope dominance disparities in our RSV infection model and have the greatest suppressive effect on the dominant $K^dM2_{82–90}$ response. The differences between the control and Treg-cell-depleted groups are statistically significant for all organs (Fig. 5). Despite the fact that RSV infects only the lungs, this effect was systemic, also affecting the balance of responses in secondary lymphoid organs.

**Treg-cell depletion increases chemokines and both type 1 and type 2 cytokine levels following RSV infection but does not change the cytokine profile of RSV-specific $CD8^+$ T cells.** Treg cells have been reported to dampen many different innate and adaptive responses (30, 31). We investigated how Treg-cell depletion affected cytokine and chemokine levels in the RSV-infected lung. Frozen, ground lung supernatants from isotype control and Treg-cell-depleted mice 7 days postinfection were shipped to Pierce (Woburn, MA) for analysis with a SearchLight proteome array. An array of chemokines (MIP-1α [macrophage inflammatory protein-1α], MIP-1β, and MCP-1 [monocyte chemotactic protein 1]), cytokines (IL-2, IL-4, IL-10, IL-13, TNF-α, and IFN-γ), and total transforming growth factor β (TGF-β) were quantitated. We found significantly higher levels of the chemokines MIP-1α, MIP-1β, and MCP-1 in the lungs of Treg-cell-depleted mice than in control mice 7 days postinfection despite finding lower numbers of RSV-specific $CD8^+$ T cells in the Treg-cell-depleted group at the day 7 time point, as mentioned previously. Higher levels of IL-2, IFN-γ, and TNF-α in addition to IL-4 indicated a general increase in cytokine production from different cell subsets. While we saw a trend for higher IL-10 in the Treg-cell-de-

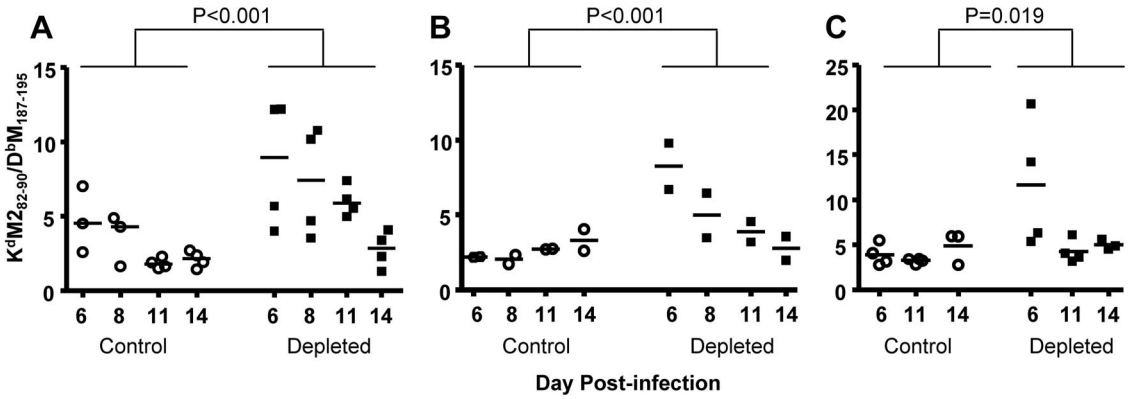


FIG. 5. Exaggeration of immunodominance disparities in anti-CD25-treated mice compared with controls. Mice were treated with 500 μg of isotype antibody (Y13-259; control) or 500 μg of PC61 antibody (depleted) intraperitoneally 3 days prior to intranasal infection with RSV. The percentage of $CD8^+$ T cells specific for the $K^dM2_{82–90}$ epitope or the $D^bM_{187–195}$ epitope was quantitated, and the dominant $K^dM2_{82–90}$ response was divided by the subdominant $D^bM_{187–195}$ response in the lungs (A), spleen (B), and mediastinal lymph node (C) at the indicated day postinfection with RSV. The mean is shown as a horizontal bar, and statistics were calculated as described in Materials and Methods.

pleted group, the difference was not statistically significant ($P = 0.055$) due to one potential outlier in the Treg-cell-depleted group (Fig. 6). There were no differences between the control and depleted groups for IL-13 or total TGF-β production (data not shown). These data suggest that Treg-cell depletion increased the overall functional activity of multiple cell types.

In order to investigate whether some of the cytokine differences seen following Treg-cell depletion were due to a difference in the response of epitope-specific $CD8^+$ T cells, we performed ICS on cell samples taken from the lung, spleen, and mediastinal lymph nodes of both the isotype control and Treg-cell-depleted groups following in vitro $M2_{82–90}$ or $M_{187–195}$ peptide stimulation. IL-2, IFN-γ, and TNF-α were measured simultaneously and after single-positive gating for each. Boolean gating was performed on FlowJo, version 8.5, to generate a functional profile for epitope-specific $CD8^+$ T cells. $K^dM2_{82–90}$ and the $D^bM_{187–195}$ epitope-specific responses are shown for the lung, spleen, and mediastinal lymph node in Fig. 7. As reported by our group and others, not all RSV-specific cells in the lung produce cytokines following peptide stimulation (3, 35). This is particularly apparent in the lungs, where cytokine production is typically observed in less than half of the dominant $K^dM2_{82–90}$ epitope-specific cells. A higher frequency of lung-derived $D^bM_{187–195}$-specific cells produce cytokines when stimulated with peptide (Fig. 7A). Most $M2_{82–90}$- or $M_{187–195}$-stimulated cells from RSV-infected lungs produce IFN-γ only, with a small fraction producing both IFN-γ and TNF-α but little to no IL-2. It is clear that the increased cytokine levels in the lung of Treg-cell-depleted mice 7 days postinfection are not entirely due to the antigen-specific $CD8^+$ T-cell responses, which are quantitatively lower in the Treg-cell-depleted lungs at this time point and are found to produce a similar cytokine profile in the isotype control and Treg-cell-depleted groups. Additionally, cytokine and chemokine levels decrease almost to background levels by 10 days postinfection when $CD8^+$ T-cell responses are near their peak (Fig. 7). More $K^dM2_{82–90}$- and $D^bM_{187–195}$-specific $CD8^+$ T cells in the spleen and mediastinal lymph node respond to peptide stimulation by cytokine production than these cell types in the lung. Additionally, RSV-specific cells are more polyfunctional in secondary lymphoid organs, with a higher percentage of responding cells producing both IFN-γ and TNF-α, IFN-γ, and IL-2 or all three cytokines simultaneously in the spleen (Fig. 7B) and the lymph node (Fig. 7C).

**Treg-cell depletion during primary infection increases the memory $CD8^+$ T-cell response to RSV.** We measured memory responses to the $K^dM2_{82–90}$ and subdominant $D^bM_{187–195}$ epitopes in the spleen 50 days after primary RSV infection with specific tetramers and for IL-2, IFN-γ, and TNF-α production following peptide stimulation. Both epitope-specific memory responses were higher in the Treg-cell-depleted group than in the isotype control, as measured by tetramer staining ($P = 0.004$ for $K^dM2_{82–90}$, and $P = 0.02$ for $D^bM_{187–195}$) (Fig. 8A). Following $M2_{82–90}$ or $M_{187–195}$ stimulation, memory cells for both epitopes were shown to be highly polyfunctional, with the majority of cells producing at least two cytokines (Fig. 8A). As was seen during primary infection, fewer $K^dM2_{82–90}$-specific cells produce cytokines than $D^bM_{187–195}$-specific cells. We addressed immunodominance disparity in the memory phase by again taking the ratio of the dominant epitope to the subdominant epitope for each mouse. The $K^dM2_{82–90}/D^bM_{187–195}$ response ratio was under 3 for both the isotype control and the Treg-cell-depleted group 50 days postinfection, with no significant difference between the groups (Fig. 8B).

## DISCUSSION

Treg cells have been found to play a role in regulation of adaptive immune response to several viruses (1, 31, 33). We are the first to describe that Treg cells are enriched in the lungs of mice infected intranasally with RSV and that they systemically regulate $CD8^+$ T-cell responses to infection. In our hybrid mouse model for RSV infection, depletion of Treg cells with the PC61 (anti-CD25) antibody has organ-specific effects. Specific $CD8^+$ T-cell responses in the lymph node and spleen are increased by depletion, yet responses in the lung are delayed at early time points following infection. The delay in adaptive immune responses in the lungs resulted in less efficient pathogen clearance and less $CD8^+$ T-cell-mediated

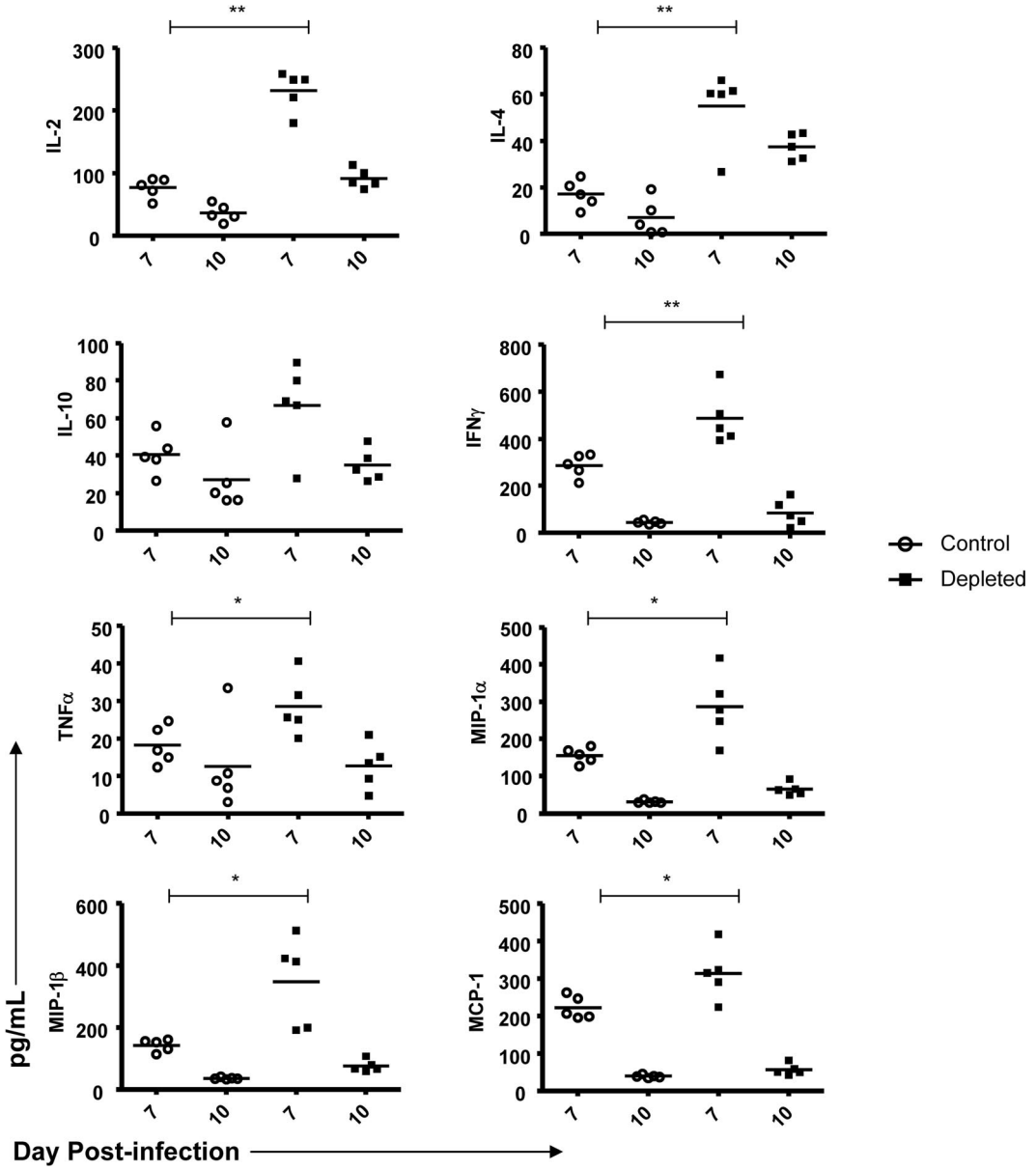


FIG. 6. Cytokine and chemokine levels in control and anti-CD25-treated lungs. The single lobe of the left lung was quick frozen in 2 ml of 10% EMEM and later ground with a mortar and pestle. Cell debris was spun out, and supernatants were sent to the SearchLight service at Pierce for blind quantitation (in pg/ml) for 11 cytokines and chemokines in each sample. IL-10, IL-13, and TGF-β results showed no significant difference between control and depleted groups. *, $P < 0.05$; **, $P < 0.01$ (two-tailed Student's $t$ test).

weight loss during early infection in the hybrid mouse model. To our knowledge, this is the first description of Treg-cell depletion resulting in less efficient clearance of a pulmonary pathogen despite higher $CD8^+$ T-cell responses in other organs. Taken together, our data show that Treg cells do not hinder, and may actually facilitate, RSV clearance from the lungs. Additionally, they were found to modulate disease and epitope dominance disparities and to dampen the memory response to the virus.

As with most experimental procedures, depletion of Treg cells with anti-CD25 antibodies is not without its caveats. Depletion of $FoxP3^+$ Treg cells by this method is decidedly incomplete (6). Further complications may occur as the high-affinity IL-2 receptor, CD25, can also be expressed on recently activated conventional T lymphocytes. Despite CD25 expression on many activated lymphocytes, higher lymphocyte responses and proliferation are typically observed following Treg-cell depletion, potentially due to stimulation through low-affinity IL-2 receptors on the same cells and an abundance of IL-2 in the absence of Treg cells (37). Throughout our studies of primary infection with RSV, we observed relatively low numbers of $CD8^+$ $CD25^+$ cells and $CD4^+$ $FoxP3^-$ $CD25^+$ cells in the lung, lymph node, and spleen, and depletion with the PC61 antibody had little effect on these populations (Fig. 2).

Two new mouse models that offer more complete depletion

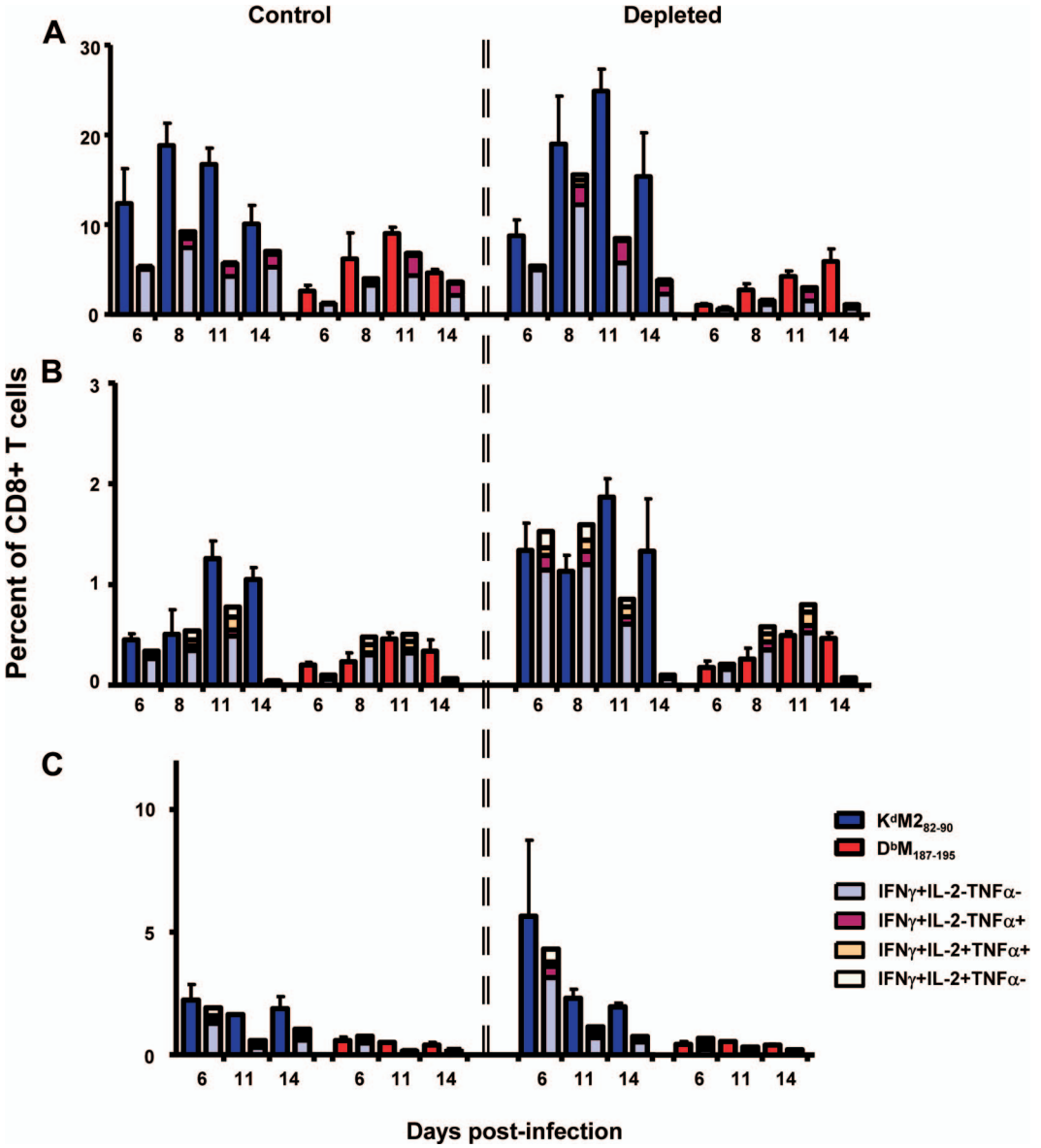


FIG. 7. Functionality of $K^dM2_{82-90}$- and $D^bM_{187-195}$-specific cells in the lung, spleen, and mediastinal lymph node. The percentage of $CD8^+$ T cells specific for the $K^dM2_{82-90}$ epitope or the $D^bM_{187-195}$ epitope was quantitated, and values are shown for each group for each day with a solid blue ($K^dM2_{82-90}$) or solid red ($D^bM_{187-195}$) histogram. Parallel samples for each mouse were incubated at 37°C in vitro with epitope-specific peptide, costimulatory antibodies, and monensin. After 5 hours, cells were surface stained with antibodies for CD3 and CD8 and then permeabilized and stained intracellularly with antibodies for IFN-γ, IL-2, and TNF-α. ICS results are shown next to the tetramer results for each group of samples from the lung (A), spleen (B), and mediastinal lymph node (C). The means of total cell numbers between treatment groups were all within 1 standard deviation. Results are representative of two experiments, with four to five mice per group per day.

of Treg cells have recently been reported (18, 20). These cleaner methods of diphtheria toxin-mediated depletion of $FoxP3^+$ T cells will soon offer new insights into the role that Treg cells play during viral infection. Of particular interest, a recent report investigating Treg-cell responses to herpes simplex virus type 2 in one of these mouse models showed a similar contradictory effect of Treg-cell depletion as that which we observed in our RSV infection model (23). Treg-cell-ablated, herpes simplex virus type 2-infected mice were found to have increased viral loads and impaired migration of antiviral effector cells to the site of infection despite robust responses in the draining lymph node. The delay in immune cell influx at the site of infection was estimated to be 2 days in Treg-cell-ablated mice, a delay similar to what we observed in the lungs of RSV-infected mice. In another parallel between our studies, Lund et al. also reported higher cytokine and chemokine responses in Treg-cell-ablated animals (23). Regulation of a wide variety of cell types and control of the cytokine and chemokine milieu following infection allow Treg cells to assume the paradoxical role of coordinating and facilitating early immune responses at the site of infection while modulating the response in peripheral lymphoid organs.

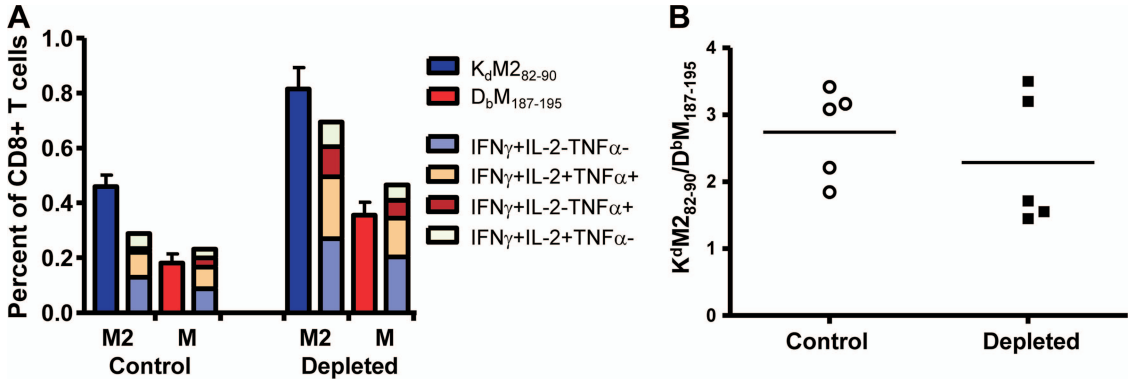


FIG. 8. Epitope-specific memory responses in control and anti-CD25-treated mice. (A) Cells were isolated from spleens of mice 50 days following infection with RSV, and the percentages of $CD8^+$ T cells specific for the $K^dM2_{82–90}$ (M2) and $D^bM_{187–195}$ (M) epitopes and T-cell function were determined by flow cytometry as described in the legend of Fig. 7. (B) The ratio of epitope-specific responses was determined by dividing the dominant M2 response by the subdominant M response.

Enhanced $CD8^+$ T-cell responses in the lung at later time points following RSV infection of the Treg-cell-depleted group may be the result of higher cytokine and chemokine production early in infection or of greater antigen persistence rather than direct suppression by Treg cells. The cytokine profiles of RSV-specific cells were similar between the control and the depleted groups for all organs, indicating that there may not be a direct effect of Treg cells on RSV-specific $CD8^+$ T-cell function. We observed modulation of the immunodominance disparity between the dominant $K^dM2_{82–90}$ and the subdominant $D^bM_{187–195}$ responses following Treg-cell depletion, but this effect seemed greatest early in infection. It is possible that the Treg cells have a greater influence on T cells that are more activated and that the dominant $CD8^+$ T cells that are probably dividing most rapidly are most affected. Later in infection and during the memory phase, the $K^dM2_{82–90}/D^bM_{187–195}$ response ratio returned to levels seen throughout the infection in control mice. The decline in epitope disparity may indicate that dominant $K^dM2_{82–90}$ cells may be more highly activated and driven to terminal effectors, leading to apoptosis, and are less likely to persist into the memory phase in the Treg-cell-depleted group. Despite a similar $K^dM2_{82–90}/D^bM_{187–195}$ ratio between the control and Treg-cell-depleted groups in the memory phase, responses to both epitopes were quantitatively higher in the Treg-cell-depleted group, indicating that the presence of Treg cells during primary infection may lower the number of RSV-specific $CD8^+$ T cells that survive into the memory phase.

Premature infants and infants under the age of 6 months are most susceptible to severe RSV disease and hospitalization for bronchiolitis, pneumonia, bronchitis, and croup (26). While initially recognized as a major health threat in infants, RSV is now recognized as a common respiratory pathogen among the immunocompromised and the elderly and accounts for up to 10,000 deaths in people over 65 in the United States each year (25). Causes of severe manifestations of RSV infection are clearly multifaceted and complex, involving both viral and host factors (reviewed in reference 5). The lungs of infected individuals can exhibit high levels of type 1 and type 2 cytokines, proinflammatory cytokines, and other immune mediators (5). Studies have shown that exaggerated type 1 or type 2 adaptive responses can be associated with a negative outcome following infection.

The role for $CD8^+$ T cells in the pathology of human RSV disease is controversial. In contrast to the immune response to RSV in the mouse, where $K^dM2_{82–90}$ is an unusually immunodominant epitope and high $CD8^+$ T-cell activity correlates directly with disease, the immunopathology of human RSV infection is more complex and more difficult to study. The immunopathology of primary infection in human infants is typically neutrophil mediated (7, 16), and the enhancement of disease following vaccination attempts in the 1960s was found to be mediated by eosinophils and immune complex deposition (17, 28). In these settings, $CD8^+$ T cells are believed to have a protective effect and not contribute to pathology. Mouse studies have shown that $CD8^+$ T-cell responses can protect against eosinophil-mediated disease after vaccination in the mouse model (15, 27, 38), and a recent human study in young infants who died during primary RSV infection suggests that RSV-mediated lower respiratory tract infections may be related to a failure to develop an adaptive cytotoxic T-cell response (42). $CD8^+$ T cells observed following RSV infection in the human are distributed in both airways and lung parenchyma (16) and can be isolated in bronchoalveolar lavage fluid but do not correlate with disease severity (13). Understanding how Treg cells modulate $CD8^+$ T-cell responses and other aspects of the immune response to RSV may help explain the hallmarks of infection in infants, such as the lack of an effective $CD8^+$ T-cell response in severe primary disease, the inability of the immune system to generate a functional memory response, and an increased likelihood to develop asthma and allergies in those who experience severe RSV disease.

## ACKNOWLEDGMENTS

This work was supported by intramural funding through the National Institute of Allergy and Infectious Diseases.

Reagents for initial experiments were provided by the NIH Tetramer Core Facility, Emory University, Atlanta, GA.

## REFERENCES

1. **Belkaid, Y.** 2008. Role of Foxp3-positive regulatory T cells during infection. Eur. J. Immunol. **38:**918–921.
2. **Belkaid, Y., and B. T. Rouse.** 2005. Natural regulatory T cells in infectious disease. Nat. Immunol. **6:**353–360.

3. **Chang, J., and T. J. Braciale.** 2002. Respiratory syncytial virus infection suppresses lung CD8$^+$ T-cell effector activity and peripheral CD8$^+$ T-cell memory in the respiratory tract. Nat. Med. **8:**54–60.
4. **Chang, J., A. Srikiatkhachorn, and T. J. Braciale.** 2001. Visualization and characterization of respiratory syncytial virus F-specific CD8(+) T cells during experimental virus infection. J. Immunol. **167:**4254–4260.
5. **Collins, P. L., and B. S. Graham.** 2008. Viral and host factors in human respiratory syncytial virus pathogenesis. J. Virol. **82:**2040–2055.
6. **Couper, K. N., D. G. Blount, J. B. de Souza, I. Suffia, Y. Belkaid, and E. M. Riley.** 2007. Incomplete depletion and rapid regeneration of Foxp3+ regulatory T cells following anti-CD25 treatment in malaria-infected mice. J. Immunol. **178:**4136–4146.
7. **Everard, M. L., A. Swarbrick, M. Wrightham, J. McIntyre, C. Dunkley, P. D. James, H. F. Sewell, and A. D. Milner.** 1994. Analysis of cells obtained by bronchial lavage of infants with respiratory syncytial virus infection. Arch. Dis. Child. **71:**428–432.
8. **Fernandez, M. A., F. K. Puttur, Y. M. Wang, W. Howden, S. I. Alexander, and C. A. Jones.** 2008. T regulatory cells contribute to the attenuated primary CD8$^+$ and CD4$^+$ T cell responses to herpes simplex virus type 2 in neonatal mice. J. Immunol. **180:**1556–1564.
9. **Furuichi, Y., H. Tokuyama, S. Ueha, M. Kurachi, F. Moriyasu, and K. Kakimi.** 2005. Depletion of CD25$^+$ CD4$^+$ T cells (Tregs) enhances the HBV-specific CD8$^+$ T cell response primed by DNA immunization. World J. Gastroenterol. **11:**3772–3777.
10. **Graham, B. S., L. A. Bunton, P. F. Wright, and D. T. Karzon.** 1991. Role of T lymphocyte subsets in the pathogenesis of primary infection and rechallenge with respiratory syncytial virus in mice. J. Clin. Investig. **88:**1026–1033.
11. **Graham, B. S., M. D. Perkins, P. F. Wright, and D. T. Karzon.** 1988. Primary respiratory syncytial virus infection in mice. J. Med. Virol. **26:**153–162.
12. **Haeryfar, S. M., R. J. DiPaolo, D. C. Tscharke, J. R. Bennink, and J. W. Yewdell.** 2005. Regulatory T cells suppress CD8$^+$ T cell responses induced by direct priming and cross-priming and moderate immunodominance disparities. J. Immunol. **174:**3344–3351.
13. **Heidema, J., M. V. Lukens, W. W. van Maren, M. E. van Dijk, H. G. Otten, A. J. van Vught, D. B. van der Werff, S. J. van Gestel, M. G. Semple, R. L. Smyth, J. L. Kimpen, and G. M. van Bleek.** 2007. CD8$^+$ T cell responses in bronchoalveolar lavage fluid and peripheral blood mononuclear cells of infants with severe primary respiratory syncytial virus infections. J. Immunol. **179:**8410–8417.
14. **Hori, S., T. Nomura, and S. Sakaguchi.** 2003. Control of regulatory T cell development by the transcription factor Foxp3. Science **299:**1057–1061.
15. **Hussell, T., C. J. Baldwin, A. O'Garra, and P. J. Openshaw.** 1997. CD8$^+$ T cells control Th2-driven pathology during pulmonary respiratory syncytial virus infection. Eur. J. Immunol. **27:**3341–3349.
16. **Johnson, J. E., R. A. Gonzales, S. J. Olson, P. F. Wright, and B. S. Graham.** 2007. The histopathology of fatal untreated human respiratory syncytial virus infection. Mod. Pathol. **20:**108–119.
17. **Johnson, T. R., and B. S. Graham.** 2004. Contribution of respiratory syncytial virus G antigenicity to vaccine-enhanced illness and the implications for severe disease during primary respiratory syncytial virus infection. Pediatr. Infect. Dis. J. **23:**S46–57.
18. **Kim, J. M., J. P. Rasmussen, and A. Y. Rudensky.** 2007. Regulatory T cells prevent catastrophic autoimmunity throughout the lifespan of mice. Nat. Immunol. **8:**191–197.
19. **Kulkarni, A. B., H. C. Morse, 3rd, J. R. Bennink, J. W. Yewdell, and B. R. Murphy.** 1993. Immunization of mice with vaccinia virus-M2 recombinant induces epitope-specific and cross-reactive K$^d$-restricted CD8$^+$ cytotoxic T cells. J. Virol. **67:**4086–4092.
20. **Lahl, K., C. Loddenkemper, C. Drouin, J. Freyer, J. Arnason, G. Eberl, A. Hamann, H. Wagner, J. Huehn, and T. Sparwasser.** 2 January 2007. Selective depletion of Foxp3$^+$ regulatory T cells induces a scurfy-like disease. J. Exp. Med. **204:**57–63. [Epub ahead of print.]
21. **Lee, S., S. A. Miller, D. W. Wright, M. T. Rock, and J. E. Crowe, Jr.** 2007. Tissue-specific regulation of CD8$^+$ T-lymphocyte immunodominance in respiratory syncytial virus infection. J. Virol. **81:**2349–2358.
22. **Lukens, M. V., E. A. Claassen, P. M. de Graaff, M. E. van Dijk, P. Hoogerhout, M. Toebes, T. N. Schumacher, R. G. van der Most, J. L. Kimpen, and G. M. van Bleek.** 2006. Characterization of the CD8$^+$ T cell responses directed against respiratory syncytial virus during primary and secondary infection in C57BL/6 mice. Virology **352:**157–168.
23. **Lund, J. M., L. Hsing, T. T. Pham, and A. Y. Rudensky.** 24 April 2008. Coordination of early protective immunity to viral infection by regulatory T cells. Science **320:**1220–1224. [Epub ahead of print.]
24. **McHugh, R. S., and E. M. Shevach.** 2002. The role of suppressor T cells in regulation of immune responses. J. Allergy Clin. Immunol. **110:**693–702.
25. **Murata, Y., and A. R. Falsey.** 2007. Respiratory syncytial virus infection in adults. Antivir. Ther. **12:**659–670.
26. **Murphy, B. R., G. A. Prince, P. L. Collins, K. Van Wyke Coelingh, R. A. Olmsted, M. K. Spriggs, R. H. Parrott, H. W. Kim, C. D. Brandt, and R. M. Chanock.** 1988. Current approaches to the development of vaccines effective against parainfluenza and respiratory syncytial viruses. Virus Res. **11:**1–15.
27. **Olson, M. R., and S. M. Varga.** 2007. CD8 T cells inhibit respiratory syncytial virus (RSV) vaccine-enhanced disease. J. Immunol. **179:**5415–5424.
28. **Polack, F. P., M. N. Teng, P. L. Collins, G. A. Prince, M. Exner, H. Regele, D. D. Lirman, R. Rabold, S. J. Hoffman, C. L. Karp, S. R. Kleeberger, M. Wills-Karp, and R. A. Karron.** 2002. A role for immune complexes in enhanced respiratory syncytial virus disease. J. Exp. Med. **196:**859–865.
29. **Quinn, K. M., F. J. Rich, L. M. Goldsack, G. W. de Lisle, B. M. Buddle, B. Delahunt, and J. R. Kirman.** 2008. Accelerating the secondary immune response by inactivating CD4(+)CD25(+) T regulatory cells prior to BCG vaccination does not enhance protection against tuberculosis. Eur. J. Immunol. **38:**695–705.
30. **Ralainirina, N., A. Poli, T. Michel, L. Poos, E. Andres, F. Hentges, and J. Zimmer.** 2007. Control of NK cell functions by CD4+ CD25+ regulatory T cells. J. Leukoc. Biol. **81:**144–153.
31. **Robertson, S. J., and K. J. Hasenkrug.** 2006. The role of virus-induced regulatory T cells in immunopathology. Springer Semin. Immunopathol. **28:**51–62.
32. **Rouse, B. T., P. P. Sarangi, and S. Suvas.** 2006. Regulatory T cells in virus infections. Immunol. Rev. **212:**272–286.
33. **Rouse, B. T., and S. Suvas.** 2007. Regulatory T cells and immunity to pathogens. Expert Opin. Biol. Ther. **7:**1301–1309.
34. **Rutigliano, J. A., M. T. Rock, A. K. Johnson, J. E. Crowe, Jr., and B. S. Graham.** 2005. Identification of an H-2D(b)-restricted CD8+ cytotoxic T lymphocyte epitope in the matrix protein of respiratory syncytial virus. Virology **337:**335–343.
35. **Rutigliano, J. A., T. J. Ruckwardt, J. E. Martin, and B. S. Graham.** 2007. Relative dominance of epitope-specific CD8$^+$ T cell responses in an F1 hybrid mouse model of respiratory syncytial virus infection. Virology **362:**314–319.
36. **Sakaguchi, S., K. Wing, and M. Miyara.** 2007. Regulatory T cells—a brief history and perspective. Eur. J. Immunol. **37**(Suppl. 1)**:**S116—S123.
37. **Sharma, R., L. Zheng, U. S. Deshmukh, W. N. Jarjour, S. S. Sung, S. M. Fu, and S. T. Ju.** 2007. A regulatory T cell-dependent novel function of CD25 (IL-2R$\alpha$) controlling memory CD8(+) T cell homeostasis. J. Immunol. **178:**1251–1255.
38. **Srikiatkhachorn, A., and T. J. Braciale.** 1997. Virus-specific CD8+ T lymphocytes downregulate T helper cell type 2 cytokine secretion and pulmonary eosinophilia during experimental murine respiratory syncytial virus infection. J. Exp. Med. **186:**421–432.
39. **Suvas, S., U. Kumaraguru, C. D. Pack, S. Lee, and B. T. Rouse.** 2003. CD4$^+$ CD25$^+$ T cells regulate virus-specific primary and memory CD8+ T cell responses. J. Exp. Med. **198:**889–901.
40. **Toka, F. N., S. Suvas, and B. T. Rouse.** 2004. CD4$^+$ CD25$^+$ T cells regulate vaccine-generated primary and memory CD8$^+$ T-cell responses against herpes simplex virus type 1. J. Virol. **78:**13082–13089.
41. **Turka, L. A., and P. T. Walsh.** 2008. IL-2 signaling and CD4+ CD25+ Foxp3+ regulatory T cells. Front. Biosci. **13:**1440–1446.
42. **Welliver, T. P., R. P. Garofalo, Y. Hosakote, K. H. Hintz, L. Avendano, K. Sanchez, L. Velozo, H. Jafri, S. Chavez-Bueno, P. L. Ogra, L. McKinney, J. L. Reed, and R. C. Welliver, Sr.** 2007. Severe human lower respiratory tract illness caused by respiratory syncytial virus and influenza virus is characterized by the absence of pulmonary cytotoxic lymphocyte responses. J. Infect. Dis. **195:**1126–1136.